The Plant Cell, Vol. 11, 849–864, May 1999, www.plantcell.org © 1999 American Society of Plant Physiologists

BUNDLE SHEATH DEFECTIVE2, a Novel Protein Required for Post-Translational Regulation of the *rbcL* Gene of Maize

Thomas P. Brutnell,[a] Ruairidh J. H. Sawers,[a] Alexandra Mant,[b] and Jane A. Langdale[a,1]

[a] Department of Plant Sciences, University of Oxford, South Parks Road, Oxford OX1 3RB, United Kingdom
[b] Department of Biological Sciences, University of Warwick, Coventry CV4 7AL, United Kingdom

The *Bundle sheath defective2* (*Bsd2*) gene is required for ribulose-1,5-bisphosphate carboxylase/oxygenase (Rubisco) accumulation in maize. Using a *Mutator* transposable element as a molecular probe, we identified a tightly linked restriction fragment length polymorphism that cosegregated with the *bsd2*-conferred phenotype. This fragment was cloned, and sequences flanking the *Mutator* insertion were used to screen a maize leaf cDNA library. Using a full-length cDNA clone isolated in this screen, we show that an abundant 0.6-kb transcript could be detected in wild-type plants but not in *bsd2-m1* plants. This 0.6-kb transcript accumulated to low levels in plants carrying an allele derived from *bsd2-m1* that conditions a less severe mutant phenotype. Taken together, these data strongly suggest that we have cloned the *Bsd2* gene. Sequence analysis of the full-length cDNA clone revealed a chloroplast targeting sequence and a region of homology shared between BSD2 and the DnaJ class of molecular chaperones. This region of homology is limited to a cysteine-rich Zn binding domain in DnaJ believed to play a role in protein–protein interactions. We show that BSD2 is targeted to the chloroplast but is not involved in general photosynthetic complex assembly or protein import. In *bsd2* mutants, we could not detect the Rubisco protein, but the chloroplast-encoded Rubisco large subunit transcript (*rbcL*) was abundant and associated with polysomes in both bundle sheath and mesophyll cells. By characterizing *Bsd2* expression patterns and analyzing the *bsd2*-conferred phenotype, we propose a model for BSD2 in the post-translational regulation of *rbcL* in maize.

INTRODUCTION

In most plants, the primary function of leaves is to fix carbon through photosynthesis. The development of photosynthetic competence within the leaf requires the coordinated expression of both nucleus- and chloroplast-encoded genes. In particular, the accumulation of the most abundant photosynthetic enzyme, ribulose-1,5-bisphosphate carboxylase/oxygenase (Rubisco), requires direct contributions from both genomes. Higher plant Rubisco is a hexadecameric enzyme composed of eight large subunits (LSUs) encoded by a single chloroplast gene, *rbcL*, and eight small subunits (SSUs) encoded by a small nuclear *RbcS* gene family (reviewed in Gutteridge and Gatenby, 1995). As chloroplast differentiation in the leaf begins, light and plastidic signals induce the accumulation of the SSU protein (Tobin and Silverthorne, 1985; Mullet, 1988; Taylor, 1989). Concomitantly, the LSU is synthesized in the stroma of the chloroplast where both LSU and SSU complexes are assembled through a chaperonin-mediated process. This intricate assembly process requires the precise coordination of nuclear and chloroplast gene activities in response to both developmental and environmental signals (Mullet, 1988; Mayfield et al., 1995).

As the name implies, Rubisco is also capable of oxygenating ribulose-1,5-bisphosphate without any net fixation of carbon. In many C_4 plants, including maize, Rubisco is restricted to the CO_2-rich environment of the bundle sheath cell, thereby driving the carboxylase reaction over the energetically wasteful oxidation reaction (Edwards and Walker, 1983). The molecular mechanisms used to localize Rubisco to bundle sheath cells have been investigated in several C_4 species, including the C_4 dicots amaranth (Wang et al., 1993) and *Atriplex rosea* (Dengler et al., 1995) and the C_4 monocot maize (Martineau and Taylor, 1985; Langdale et al., 1988b). In these plants, transcripts and proteins encoded by both *rbcL* and *RbcS* are present in both bundle sheath and mesophyll cells of dark-grown plants and in young undifferentiated leaf tissue. In amaranth, the compartmentalization of Rubisco occurs relatively late in development, as leaves undergo the metabolic transition from carbon sink to carbon source (Wang et al., 1993). In contrast, bundle sheath cell–specific Rubisco accumulation in *A. rosea*, another C_4 dicot, occurs very early in leaf development, before the maturation of bundle sheath cells (Dengler et al., 1995). In maize, the cell-specific localization of Rubisco appears to be mediated

[1] To whom correspondence should be addressed. E-mail jane.langdale@plants.ox.ac.uk; fax 44-1865275147.

by a light-dependent developmental signal (Langdale et al., 1988b). These species-specific differences in Rubisco accumulation patterns may reflect different underlying genetic mechanisms that were exploited during the polyphyletic evolution of the C_4 pathway (Moore, 1982).

Previous studies with maize have indicated that both transcriptional and post-transcriptional controls mediate bundle sheath cell–specific Rubisco accumulation in this species (Schäffner and Sheen, 1991; Meierhoff and Westhoff, 1993; Kubicki et al., 1994). For example, by using in vitro transcriptional run-on assays, it was shown that *rbcL* is more actively transcribed in bundle sheath than in mesophyll cells (Kubicki et al., 1994). However, the differences in transcription rate could not fully account for the differences in steady state levels of the transcript between the two cell types, indicating that post-transcriptional controls are also involved. Similarly, regulatory elements have been defined in the *RbcS* promoter that act to suppress *RbcS* gene expression in mesophyll cells (Schäffner and Sheen, 1991; Viret et al., 1994), yet these *RbcS* promoter fragments are still capable of driving low-level reporter gene expression in mesophyll cells. Furthermore, nuclear run-on experiments have demostrated low-level *RbcS* transcriptional activity in mesophyll cell protoplasts (Schäffner and Sheen, 1991). Therefore, post-transcriptional mechanisms must also be involved in *RbcS* gene regulation (Schäffner and Sheen, 1991; Viret et al., 1994).

In addition to transcriptional control, translational and/or post-translational controls also may regulate Rubisco accumulation patterns. For example, LSU protein synthesis was detected in isolated mesophyll cell chloroplasts (Meierhoff and Westhoff, 1993), suggesting that *rbcL* may be translated in mature mesophyll cells. Together, these data suggest that a combination of mechanisms acts to regulate Rubisco accumulation in maize.

Despite the extensive characterization of C_4 photosynthetic enzyme accumulation profiles in different C_4 plants, the intracellular and intercellular signaling mechanisms involved in establishing these patterns have remained elusive (reviewed in Brutnell and Langdale, 1998). To identify components of these signaling pathways, mutagenized maize populations were screened for mutations that specifically disrupt photosynthetic enzyme accumulation patterns in either bundle sheath or mesophyll cells (Langdale et al., 1995). Characterization of one of these mutants, *bundle sheath defective2-mutable1* (*bsd2-m1*), has shown that the *Bsd2* gene product regulates Rubisco accumulation; mutant plants fail to accumulate either the SSU or LSU protein at any time during development (Roth et al., 1996). In contrast, all of the other nuclear-encoded C_4 photosynthetic enzymes examined accumulate to wild-type levels. Because *RbcS* transcripts accumulate in the appropriate spatial and temporal patterns in the mutant, yet *rbcL* transcripts accumulate ectopically, we proposed that the primary defect in *bsd2* mutants is a failure to regulate *rbcL* gene expression. The misregulation of *rbcL* prevents the accumulation of Rubisco holoenzyme, and no photosynthesis occurs. Consequently, bundle sheath chloroplasts swell, and internal thylakoid membranes break down in the light. Interestingly, mesophyll cell chloroplasts remain intact (Roth et al., 1996).

In this study, we used the transposon-induced allele *bsd2-m1* to clone the *Bsd2* gene. We show that the gene product has features of a cysteine-rich Zn binding domain found in DnaJ-like proteins and that the protein is targeted to the chloroplast. A detailed analysis of chloroplast gene expression patterns during leaf development in both wild-type and mutant plants has led us to propose a model whereby BSD2 acts as a post-translational regulator of LSU accumulation.

RESULTS

Structure and Characterization of the *bsd2* Locus

Our previous phenotypic characterization of the *bsd2* mutant suggested that the BSD2 product regulates *rbcL* gene expression. To gain insight into how this function may be achieved and to clone the *Bsd2* gene, we used the somatically unstable *bsd2-m1* mutant allele (Roth et al., 1996). The *bsd2-m1* allele was first identified as a variegated pale green plant in genetic screens of active *Mutator* (*Mu*) lines (see Methods). The instability of the phenotype of the *bsd2-m1* mutant, together with the fact that it was isolated from active *Mu* lines, strongly suggested that a *Mu* transposable element was inserted at the *bsd2* locus.

Because the *Mu* family of transposable elements is extremely diverse (Chandler and Hardeman, 1992), several gene-specific *Mu* fragments were used in DNA gel blot analyses to identify a band that cosegregated with the *bsd2-m1* mutant phenotype (see Methods). As shown in Figure 1, a 7.8-kb *Mu8*-containing SstI restriction fragment was detected in mutant individuals (Figure 1A, lanes 7 to 9) that segregated in the wild-type siblings (Figure 1A, lanes 3 to 6). Significantly, this fragment was absent in the progenitor lines from which *bsd2-m1* plants were generated (Figure 1A, lanes 1 and 2). Further restriction digests of genomic DNA identified a 1.8-kb *Mu8*-hybridizing PstI fragment that also cosegregated with the mutant allele (data not shown). This 1.8-kb fragment was cloned into a plasmid vector (pTBP6), and sequences 5′ to the *Mu* element were amplified by polymerase chain reaction (PCR) (Bsd2.1; Figure 1C). As shown in Figure 1B, this fragment hybridized with the 7.8-kb SstI fragment identified by *Mu8* sequences in *bsd2* mutants and to an 8.2-kb fragment in wild-type individuals. In the progenitor lines, either a 6.4-kb fragment, which was not present in segregating F_2 populations, or an 8.2-kb fragment was detected.

These data suggest that the 7.8-kb fragment detected in *bsd2-m1* mutant plants represents the insertion of a 1.4-kb *Mu8* element into the 6.4-kb SstI fragment of the P_M progenitor

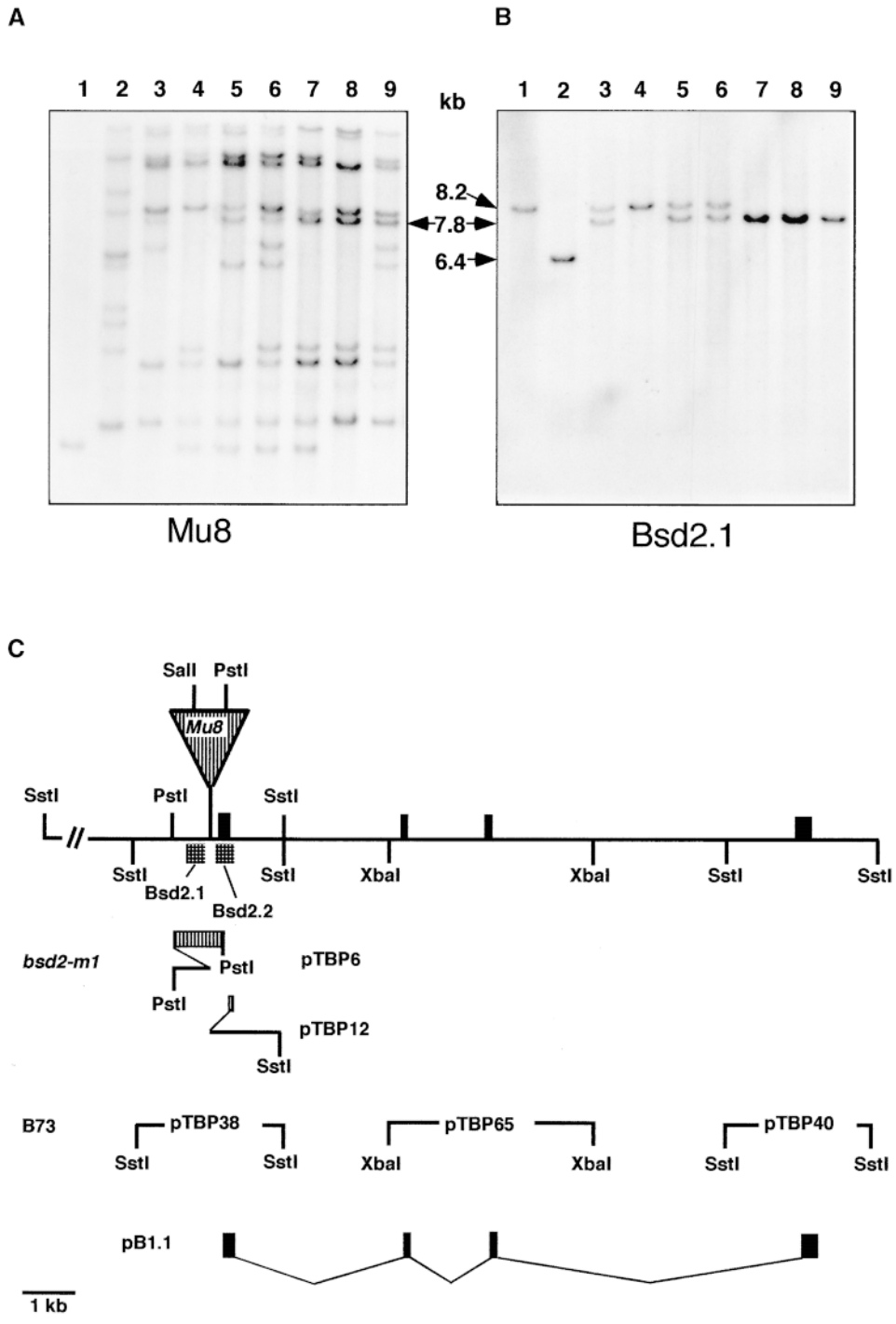

Figure 1. Structure of the *Bsd2* Gene.

(A) DNA gel blot analysis of a segregating *bsd2-m1* family hybridized with a *Mu8*-specific fragment. DNA from progenitor lines P_L and P_M (lanes 1 and 2, respectively) or from sibling wild-type plants (lanes 3 to 6) and *bsd2* mutants (lanes 7 to 9) was digested with SstI and fractionated on an 0.8% agarose gel before transfer to a nylon membrane. DNA fragment lengths are indicated by arrows.

(B) The same filter was used as in **(A)** but rehybridized with a *Bsd2*-specific fragment, Bsd2.1.

(C) Schematic representation of the *bsd2* locus. Restriction sites present in the *bsd2-m1* allele are shown above the line, and those present in the wild-type *Bsd2* allele from B73 are shown below the line. The *Bsd2* gene contains four exons, shown as filled boxes. The *Bsd2*-specific fragments used as probes are represented by cross-hatched boxes. *Mu8* sequences are shown as boxed vertical lines and are present in clones pTBP6 and pTBP12. Genomic fragments containing *Bsd2* exon sequences from B73 are also shown (pTBP38, pTBP65, and pTBP40) along with the cDNA clone (pB1.1) used in subsequent RNA gel blot analysis.

line. Wild-type individuals were either heterozygous for this *Mu*-containing fragment (Figure 1B, lanes 3, 5, and 6) or homozygous for the 8.2-kb SstI fragment present in the other parental line, P_L (Figure 1B, lane 4). DNA gel blot analysis showed that all mutant individuals examined (34 plants) were homozygous for the 7.8-kb SstI fragment, whereas the wild-type individuals examined (20 plants) were either heterozygous for the 7.8-kb band or homozygous for the 8.2-kb band (data not shown). This tight linkage (<1.5 map units) of a *Mu8*-containing restriction fragment with the somatically unstable *bsd2-m1* mutant phenotype suggested that we had cloned sequences within the *Bsd2* gene.

To elucidate the structure of the *bsd2-m1* allele and to examine the expression of the putative *Bsd2* gene, we cloned and characterized additional genomic sequences. RNA gel blot analysis of total RNA probed with Bsd2.1 (see Figure 1C) failed to identify a transcript in wild-type or *bsd2-m1* individuals (data not shown). However, further genomic restriction mapping identified a 2.8-kb SstI-SalI *Mu8*-hybridizing fragment that was also linked to the *bsd2-m1* mutant allele. A PCR-generated fragment (see Methods) derived from this allele was subcloned (pTBP12) and used to generate a fragment 3′ to *Mu8* sequences (Bsd2.2) (see Figure 1C). Gel blot analysis of total RNA showed that Bsd2.2 detected a 0.6-kb transcript in wild-type individuals that was not detectable in *bsd2* mutants (data not shown), suggesting that *Bsd2* coding sequences had been cloned. The Bsd2.2 fragment was used to screen a maize leaf cDNA library, and several cDNA clones were isolated. One of the longest clones identified (pB1.1) was used to isolate several genomic fragments encompassing the *Bsd2* coding region from a wild-type B73 inbred line (see Methods). Restriction mapping of these fragments together with gel blot analysis of genomic DNA under low-stringency conditions indicated that *Bsd2* is a single-copy gene in maize (data not shown). These data are summarized in Figure 1C. Surprisingly, the 0.6 kb of *Bsd2* coding sequence spans nearly 12 kb of genomic sequence.

The tight linkage of a *Mu* transposon with the *bsd2*-conferred phenotype and the absence of the 0.6-kb transcript in mutant plants suggested that *Bsd2* sequences had been cloned. However, the possibility remained that the *Mu*-containing restriction fragment represented a tightly linked *Mu* insertion that is not responsible for the mutant phenotype. To eliminate this possibility, we tried to identify additional mutant alleles of *bsd2* by using both reverse genetic and directed tagging strategies (see Methods). Unfortunately, neither strategy was effective in identifying another *Mu*-induced *bsd2* allele. However, we identified a novel mutant phenotype in a line derived from *bsd2-m1*. As mentioned previously, *bsd2-m1* was first identified as conditioning a variegated leaf phenotype. When these plants were outcrossed to several different inbred lines and selfed, only stable mutant phenotypes segregated in the F_2 progeny. This stable mutant phenotype was associated with an absence of *Mu* activity, as monitored by the lack of spots in kernels carrying the *bz-mum9* allele (Chomet et al., 1991). After two generations of backcrossing into *Mu*-active lines followed by self-pollination, several families of plants carrying the *bsd2-m1* allele were identified that displayed a novel mutant phenotype (Figure 2A). These plants expressed low levels of *Mu* activity (i.e., display few spots in the aleurone of the kernel) and had slightly pale green, grainy leaves. Electron micrographs of third leaf sections (Figure 2A) indicated that this grainy appearance in the leaf is due to the presence of both phenotypically wild-type and *bsd2-m1*–like mutant bundle sheath cell chloroplasts in these intermediate or *bsd2-weak* (*bsd2-w*) plants.

DNA gel blot analysis using *bsd2-w* plants indicated that the novel phenotype was not due to the excision or rearrangement of the *Mu8* insertion from the 7.8-kb SstI fragment found in *bsd2-m1* plants (data not shown). However, RNA gel blot analysis indicated that the putative 0.6-kb *Bsd2* transcript accumulated to low levels in *bsd2-w* plants (Figure 2B). Thus, a partial restoration of the wild-type phenotype was associated with an increase in the levels of the 0.6-kb transcript. Furthermore, this suppression of the mutant phenotype was strictly correlated with an increase in *Mu* activity throughout the genome. As such, the *bsd2-w* alleles are likely to represent *Mu*-suppressible alleles of *bsd2-m1*. *Mu* suppression refers to a change in phenotype conditioned by a *Mu*-induced allele corresponding to a change in the activity of *Mu* elements in the genome (Martienssen et al., 1990; Greene et al., 1994; Fowler et al., 1996). Thus, the strict correlation of mutant phenotype to *Mu* activity in the genome together with our finding of complete linkage between a *Mu8* insertion and the *bsd2-m1*–conferred phenotype strongly suggest that we have cloned the *Bsd2* gene.

To define further the *bsd2* locus, we sequenced both cDNA (pB1.1) and genomic clones (pTBP38, pTBP65, and pTBP40). As shown in Figure 3A, *Bsd2* encodes an ~0.6-kb transcript. However, a heterogeneously sized population of cDNA clones was isolated. The clones differed in both putative transcription start sites and polyadenylation sites. One explanation for the heterogeneous transcript start sites is the absence of a strong consensus TATA box motif in the *Bsd2* gene. Alternatively, the heterogeneity in 5′ end sequences may have been an artifact of cDNA synthesis resulting from prematurely terminated cDNA transcripts during library construction. To address this possibility, we used a modified 5′ rapid amplification of cDNA ends procedure (Troutt et al., 1992) to map the 5′ transcription start site (see Methods). Results of this analysis indicated that several start sites are used (arrows in Figure 3A). Some of these transcription start sites were identical to the most 5′ sequences found in cDNA clones, indicating that multiple transcription start sites are used in *Bsd2* transcription. Similarly, multiple polyadenylation sites were identified at the 3′ end of the gene (Figure 3A, underlined sequences), suggesting that different polyadenylation signals are recognized during *Bsd2* transcriptional processing.

As shown in Figure 3B, *Bsd2* is predicted to encode a

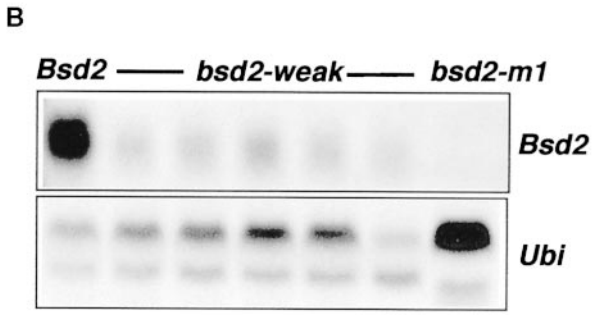

Figure 2. Characterization of the *bsd2-w* Allele.

(A) Phenotypes conditioned by wild-type (left), *bsd2-w* (center), and *bsd2-m1* (right) alleles. At top is the variegation pattern in kernels carrying the *bz-mum9* allele. At center (third leaf) and bottom (electron microscopy of third leaf sections), the corresponding leaf phenotypes associated with changes in *Mu* activity in the genome are shown. Bundle sheath (BS) and mesophyll (M) cells are indicated. The arrowheads show mutant (filled arrowhead) and phenotypically wild-type (open arrowhead) chloroplasts present in the adjacent bundle sheath cells of *bsd2-w* plants. Bars = 2 μm.

(B) RNA gel blot analysis of *Bsd2* transcript accumulation patterns conditioned by *bsd2-w* alleles. Total RNA was isolated from the third leaf of a wild-type (*Bsd2*) plant, five *bsd2-w* individuals, and a *bsd2-m1* plant. Approximately 5 μg of RNA was used for each lane. Filters were hybridized with the *Bsd2* (pB1.1) gene-specific fragment, as indicated. A maize ubiquitin fragment (*Ubi*) was used as a loading control.

129–amino acid protein. Database searches identified both a putative chloroplast targeting signal and a region that shares similarity with the cysteine-rich region (CRR) found in some members of the DnaJ class of molecular chaperones (Kelley, 1998). In bacterial DnaJ, this region forms two Zn fingers that are likely to be involved in protein–protein interactions (Banecki et al., 1996; Szabo et al., 1996). However, the predicted BSD2 protein lacks the N-terminal J domain that defines the DnaJ class of molecular chaperones as well as a cysteine- and phenylalanine-rich internal domain and large C terminus shared in most DnaJ proteins (Kelley, 1998) (Figure 3C). Nevertheless, searches of GenBank databases revealed both rice and Arabidopsis expressed sequence tags (ESTs) that share notable sequence similarity with the *Bsd2* gene. In particular, a putative rice gene that is predicted to share >58% amino acid sequence identity with BSD2 was identified, as was a putative Arabidopsis gene that is predicted to share >64% amino acid identity in the CRR. The striking sequence conservation between the *Bsd2* gene and the EST sequences, particularly in the CRR, suggests that this region is essential for BSD2 function. Searches of sequence databases identified only plant genes that share identity with *Bsd2*. This is somewhat surprising given the abundance of *Bsd2* transcripts (see below) and the striking similarity between the rice, maize, and Arabidopsis clones. These findings suggest that BSD2-like proteins define a new class of small cysteine-rich proteins that may be unique to plants.

BSD2 Is Targeted to the Chloroplast

Both the phenotypic characterization of *bsd2* mutants (Roth et al., 1996) and sequence analysis of the *Bsd2* gene suggest that BSD2 is targeted to the chloroplast. To test this prediction, we performed an in vitro import assay using isolated pea chloroplasts. A full-length cDNA clone was first transcribed with T3 RNA polymerase. A wheat germ cell-free lysate was then used to translate the mRNA in the presence of tritiated leucine (Figure 4, lane 1). Incubation of the product with intact chloroplasts in the presence of ATP resulted in import and processing of the precursor protein to a peptide of ~10 kD (Figure 4, lane 2). Treatment of the chloroplasts with thermolysin, which degrades unbound or unprotected proteins from the chloroplast envelope, allowed the size of the processed protected protein to be unequivocally determined (Figure 4, lane 3). Subsequent fractionation

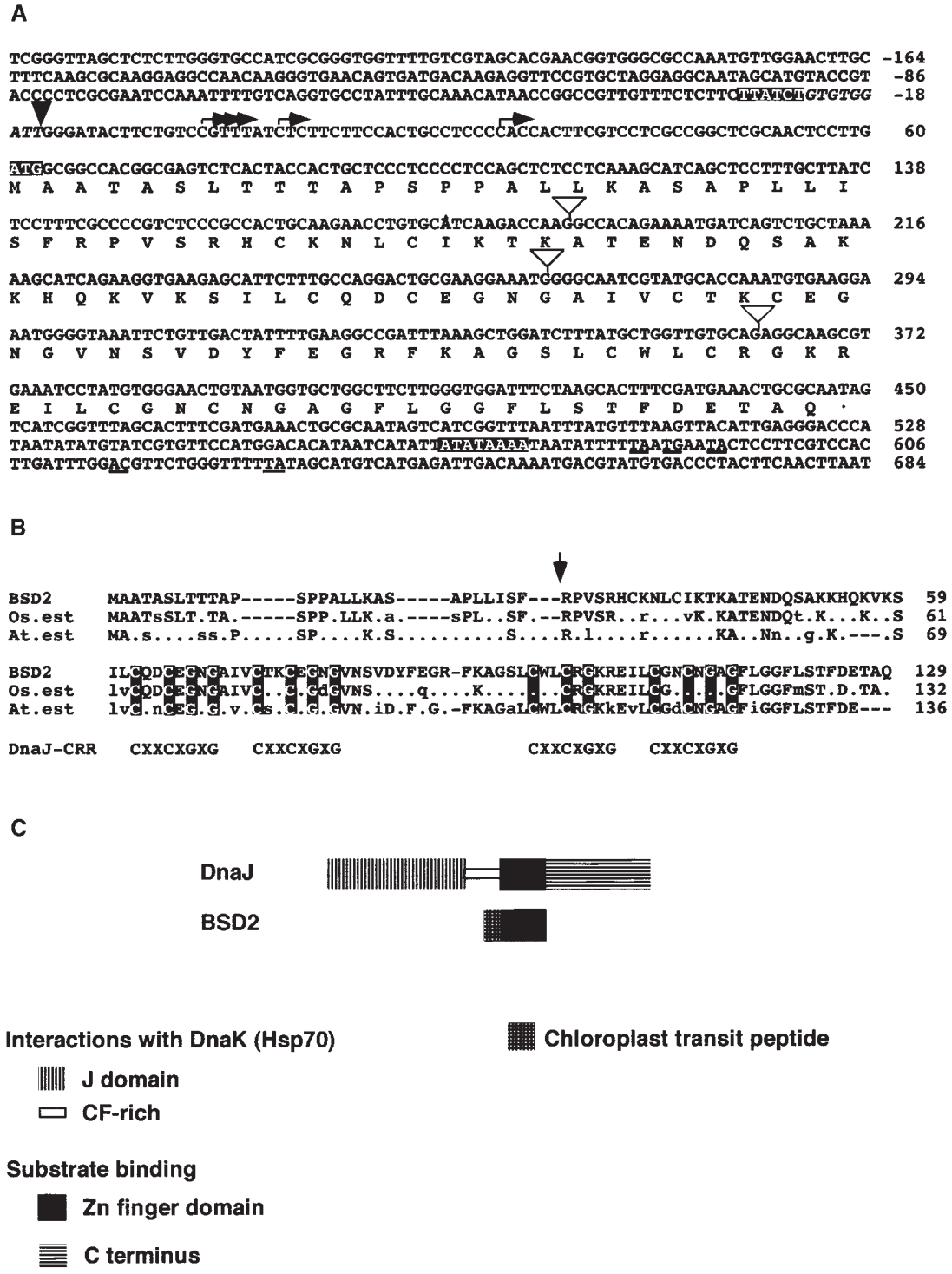

Figure 3. Sequence Analysis of the *Bsd2* Gene.

(A) cDNA and deduced amino acid sequence of *Bsd2* shown with 5′ and 3′ genomic sequences (GenBank accession number AF126742). Mapped transcription start sites are indicated by arrows. The putative TATA box and polyadenylation sites are highlighted. The position of the *Mu* insertion is shown as a filled triangle, and the 9-bp duplication generated upon insertion is shown in italics. Introns are denoted with open triangles. Sites of polyadenylation are underlined.

of chloroplasts showed that BSD2 localizes to the stromal compartment of the chloroplast (Figure 4, lanes 4 and 5).

Expression Profile of the *Bsd2* Gene

To examine the accumulation profile of *Bsd2* transcripts in wild-type and *bsd2* plants, we performed RNA gel blot analysis. As shown in Figure 5A, *Bsd2* transcripts were localized to shoot tissues and were relatively abundant in etiolated, light-shifted, and young (plastochron 1 to 5) leaves of wild-type plants but were present at greatly reduced levels in the mutant. The presence of even very low levels of *Bsd2* transcript in *bsd2* mutants was unexpected because the *Mu8* insertion in *bsd2-m1* (see Figure 3A) displaces the promoter elements ~1.4 kb upstream from the major transcription start site. However, previous studies with *Mu* (Barkan and Martienssen, 1991) have shown that weak promoter elements exist in the terminal inverted repeats of the *Mu* transposon. These elements may be responsible for the very low levels of *Bsd2* gene expression seen in mutant plants. Further experiments are under way to examine this possibility.

If the *Bsd2* gene has a direct role in regulating *rbcL* gene expression, it may be expected to show a similar expression profile to the *rbcL* gene. To examine this possibility, we compared the accumulation pattern of *Bsd2* transcripts with the pattern of *rbcL* transcript accumulation throughout the leaf blade and sheath. In the maize leaf, a developmental gradient exists such that older tissue near the tip of the leaf differentiates before younger tissue located near the base. The accumulation levels of *rbcL* transcripts are tightly coordinated with this developmental gradient (Langdale et al., 1988a), with levels peaking near the base of the leaf and declining toward the tip (Figure 5B). The accumulation profile of *Bsd2* was similar to that of *rbcL* in the leaf sheath and in the lower half of the leaf blade. However, in contrast to the *rbcL* transcripts, *Bsd2* transcripts accumulated to the highest level at the middle and tip of the leaf blade. Interestingly, this profile of *Bsd2* transcript accumulation is more similar to the accumulation profile of the LSU protein, which gradually increases from the base to the tip of the leaf (Langdale et al., 1987).

Our previous characterization of *bsd2* mutants suggested that BSD2 acts in both bundle sheath and mesophyll cells to regulate *rbcL* transcript accumulation patterns (Roth et al., 1996). To examine *Bsd2* gene expression in these two cell types, we isolated bundle sheath cell strands and mesophyll cell protoplasts from light-grown wild-type plants (see Methods). One limitation of this procedure is that it involves an enzymatic digestion of small leaf strips in buffer to release mesophyll cell protoplasts (Sheen and Bogorad, 1985). As shown in Figure 5C, simply incubating tissue strips in this buffer without enzyme resulted in an increased accumulation of phosphoenolpyruvate carboxylase (*Ppc1*) transcripts relative to untreated leaves that were frozen immediately in liquid nitrogen after harvesting. Nevertheless, the cell-specific localization of *Ppc1* in mesophyll cells and *RbcS* in bundle sheath cells was maintained throughout the procedure, thus providing a reliable method for examining bundle sheath and mesophyll cell accumulation profiles (Sheen and Bogorad, 1985; Meierhoff and Westhoff, 1993). As shown in Figure 5C, *Bsd2* transcripts were detectable in RNA isolated from both bundle sheath and mesophyll cells. Furthermore, the mesophyll cell isolation procedure did not seem to increase *Bsd2* expression levels (cf. lanes TS and T in Figure 5C), suggesting that *Bsd2* transcripts accumulated to similar levels in both bundle sheath and mesophyll cells. Together, these expression studies demonstrate a developmental and tissue-specific accumulation pattern for *Bsd2* transcripts that is consistent with the suggestion that BSD2 regulates *rbcL* transcript and/or LSU protein accumulation patterns in both bundle sheath and mesophyll cells.

BSD2 Is Not a Component of the Light Signal Transduction Pathway

As we have suggested, BSD2 appears to regulate *rbcL* gene expression. However, the BSD2 protein may play an indirect role in this process. For example, in dark-grown wild-type plants, *rbcL* normally accumulates in both bundle sheath and mesophyll cells (Nelson et al., 1984; Sheen and Bogorad, 1985, 1986b; Langdale et al., 1988b). Thus, the ectopic accumulation of *rbcL* in mesophyll cells of light-grown *bsd2* plants (Roth et al., 1996) may result from a block in light perception or signaling mechanisms. To look at this possibility, we examined the light-responsive accumulation of both nucleus- and chloroplast-encoded transcripts in *bsd2* and

Figure 3. (continued).

(B) Protein alignment (MSA 2.1, http://www.ibc.wustl.edu/msa/man.html) of BSD2 with putative protein products encoded by ESTs . Five Arabidopsis ESTs (GenBank accession numbers H36126, H37096, H35986, T45013, and T44950) were used to generate a contiguous sequence (At.est) with obvious homology to *Bsd2*. Amino acids conserved between BSD2 and the putative rice (Os.est; GenBank accession number D48303) and Arabidopsis proteins (At.est) are shown in capital letters, and similar residues are shown in lowercase letters. Dashes indicate gaps, and dots indicate dissimilar amino acids. Conserved residues in the CXXCXGXG motif repeated four times in DnaJ are highlighted. The putative processing site of the chloroplast transit peptide is marked by an arrow.

(C) A comparison of DnaJ structural motifs with BSD2. CF-rich, cysteine- and phenylalanine-rich domain.

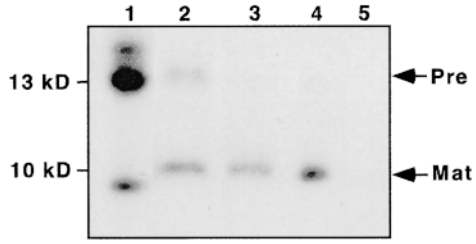

Figure 4. Chloroplast Import and Processing of the in Vitro–Synthesized BSD2 Protein in Isolated Pea Chloroplasts.

Labeled protein products of an in vitro translation reaction (lane 1) were incubated with isolated pea chloroplasts, as described in Methods. After the import incubation, chloroplasts were washed and analyzed either directly (lane 2) or after thermolysin treatment (lane 3). Chloroplasts containing processed BSD2 protein were fractionated into stromal (lane 4) and thylakoid (lane 5) compartments. The unprocessed precursor (Pre) and mature (Mat) BSD2 protein migrated at 13 and 10 kD, respectively. The ~9-kD band present in lane 1 may represent a BSD2 degradation product or result from internal initiation or premature termination within the *Bsd2* transcript.

wild-type individuals. Transcript accumulation profiles for both *Cab*, which encodes the chlorophyll *a*/*b* binding protein of light harvesting complex II (LHCPII; Sheen and Bogorad, 1986a), and *Por*, which encodes the NADPH:protochlorophyllide oxidoreductase that predominates in dark-grown tissue (PORA; Santel and Apel, 1981), were identical in wild-type and mutant plants (Figure 6). As shown, very low levels of *Cab* transcript were detected in dark-grown tissue, but high levels were detected in light-shifted tissues. Conversely, *Por* transcript levels were higher in the dark-grown than in light-shifted plants. Transcript accumulation patterns for *Por*, *Cab*, and *RbcS* have been previously shown to be mediated by phytochrome (Tobin and Silverthorne, 1985; Reinbothe et al., 1996). Therefore, because the *bsd2* mutation does not impair the light-mediated regulation of these genes (Figure 6; Roth et al., 1996), BSD2 is unlikely to be a component of the phytochrome signal transduction pathway.

To examine the role of BSD2 in mediating light-induced changes in chloroplast gene expression, we compared levels of *rbcL* and *psbA* transcripts between wild-type and mutant plants (Figure 6). In contrast to wild-type seedlings, which showed a light-induced increase in *rbcL* transcript levels, the levels of *rbcL* transcript in *bsd2* mutants were similar in both the dark-grown and light-shifted seedlings (Figure 6). The increased levels of *rbcL* transcript in dark-grown mutant seedlings compared with those in dark-grown wild-type seedlings may have resulted from either a specific increase in *rbcL* transcription rate or an increase in *rbcL* transcript stability. Alternatively, *bsd2* mutants may show a general increase in chloroplast transcription rate or transcript stability in the dark. To look at this latter possibility, we examined *psbA* transcript levels. As shown in Figure 6, levels of *psbA* transcripts were similar in wild-type and mutant plants under both light regimes, indicating that misregulation may be specific to the *rbcL* gene. Preliminary results suggest that the light regulation of the chloroplast-encoded *psaA* and *psaB* genes is also unaffected by the *bsd2* mutation (data not shown). These results suggest that BSD2 does

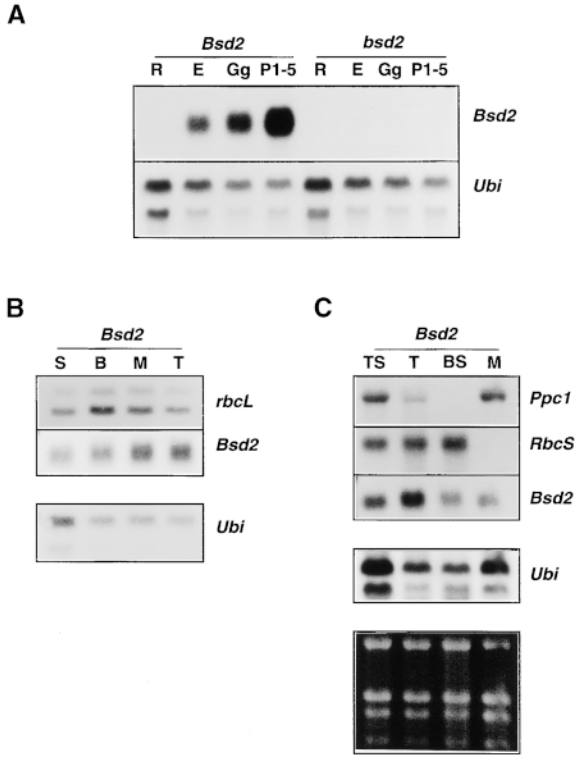

Figure 5. RNA Gel Blot Analysis of *Bsd2* Expression Patterns.

Total RNA was isolated from wild-type (*Bsd2*) or mutant (*bsd2*) plants, and ~5 μg was used for each lane. Filters were hybridized with *Bsd2* (pB1.1), *rbcL*, *RbcS*, or *Ppc1* gene–specific fragments, as indicated. A maize ubiquitin fragment (*Ubi*) was used as a loading control.

(A) Comparison of *Bsd2* transcript accumulation patterns in roots (R), etiolated shoots (E), greening shoots (Gg), and young primordia (P1-5) of wild-type and *bsd2* plants.

(B) Hybridization to RNA from third leaves of germinating light-grown seedlings divided into sheath (S), base (B; proximal third of leaf), middle (M; middle third), and tip (T; distal third) sections.

(C) Hybridization to RNA isolated from purified bundle sheath strands (BS) and mesophyll cell protoplasts (M). RNA was also isolated from the third leaf of total leaf tissue (T) and from leaf tissue incubated in the protoplast buffer without enzyme (TS). As an additional loading control, an ethidium bromide–stained gel is shown in the bottom panel, because ubiquitin (*Ubi*) expression is induced during the isolation of mesophyll cell protoplasts.

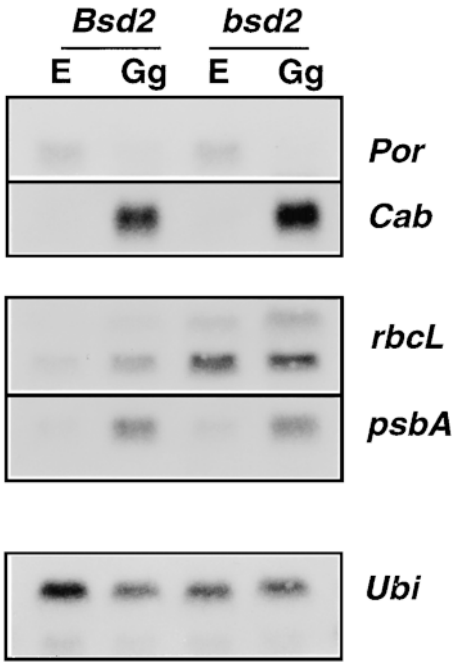

Figure 6. Light-Regulated Gene Expression in Wild-Type and *bsd2* Plants.

RNA was isolated from etiolated (E) or greening (Gg) wild-type *(Bsd2)* and mutant *(bsd2)* plants. Filters were probed with gene-specific fragments of *Por*, *Cab*, *rbcL*, and *psbA*, as indicated. A maize ubiquitin fragment (*Ubi*) was used as a loading control.

not play a direct role in light signal transduction but that the protein does regulate both environmental (Figure 6) and developmental (Roth et al., 1996) changes in *rbcL* transcript accumulation patterns.

rbcL Transcripts Are Associated with Polysomes in Leaves of *bsd2* Plants

To characterize further the role of BSD2 in *rbcL* gene regulation, we examined the association of *rbcL* transcripts with polysomes in wild-type and *bsd2* plants. Transcripts were fractionated on 15 to 45% sucrose gradients, on the basis that transcripts associated with polysomes have higher sedimentation constants than do monosomes or free RNA. The proportion of polysome-associated to unassociated transcripts provides a means to examine the efficiency of translation initiation and elongation (Barkan, 1993). As shown in Figure 7A, *rbcL* and *atpB* transcripts from wild-type and mutant plants sedimented at similar rates. Furthermore, the primary 1.8-kb *rbcL* transcript appeared to be processed correctly into a 1.6-kb transcript, and both transcripts associated with polysomes in *bsd2* mutants. The association of *rbcL* transcripts with large polysomes in the mutant plants indicated that BSD2 is unlikely to play a role in translation initiation or the early steps of elongation (see Klein et al., 1988). Thus, the failure to accumulate LSU protein in *bsd2* mutants is probably due to a post-translational defect in LSU stability or in Rubisco assembly.

The analysis of several *high chlorophyll fluorescence* mutants in maize has indicated that *rbcL* transcripts associated with polysomes are more stable than are unassociated transcripts (Barkan, 1993). Thus, the ectopic accumulation of *rbcL* transcripts in mesophyll cells of *bsd2-m1* mutants may be due to an increase in polysome-associated transcripts relative to the wild type. To address this possibility, we isolated mesophyll cell protoplasts from wild-type and *bsd2-m1* mutant leaves (see Methods), and we fractionated transcripts

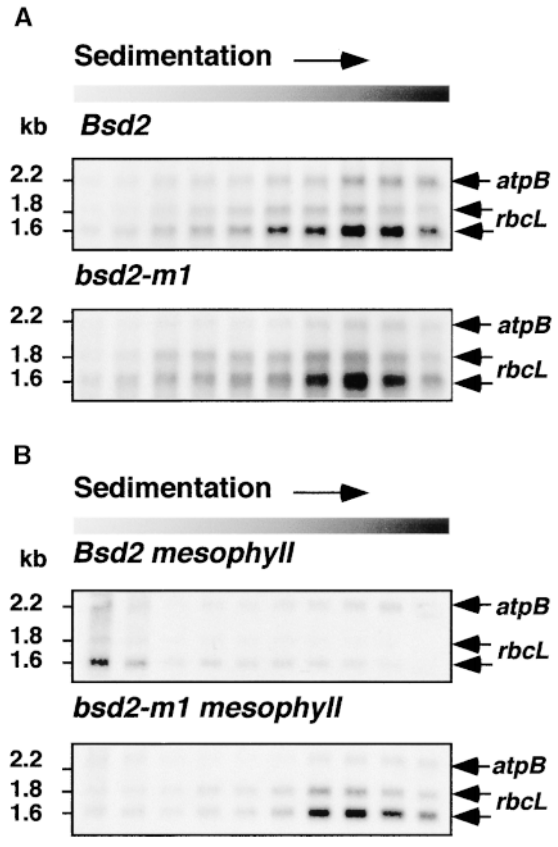

Figure 7. Association of *rbcL* and *atpB* Transcripts with Polysomes.

Protein extracts were fractionated on sucrose gradients, and 10 fractions of equal volume were collected. RNA from wild-type (top) and mutant (bottom) plants was precipitated and fractionated on 1.5% agarose gels before transfer to membranes. Blots were hybridized with a fragment that recognizes both *rbcL* and *atpB* sequences. RNA transcript lengths are indicated at left.

(A) RNA isolated from seedling tissue.

(B) RNA isolated from mesophyll cell protoplasts.

on sucrose gradients. As shown in Figure 7B, the low levels of *rbcL* transcript that accumulated in wild-type mesophyll cells were mostly unassociated with polysomes. However, the majority of *rbcL* transcripts that accumulated in *bsd2-m1* mesophyll cells were associated with ribosomes. These findings suggest that *rbcL* transcripts accumulate ectopically in mesophyll cells of *bsd2-m1* plants because they are stabilized through an association with ribosomes.

Plastid Protein Synthesis and Complex Assembly Are Not Disrupted in *bsd2-m1* Plants

Having established a role for BSD2 in the translational or post-translational regulation of LSU, it was necessary to examine the effect of the *bsd2* mutation on general chloroplast translational processing and on the assembly of photosynthetic complexes. Previous studies in maize have shown that the stability of the chloroplast ATP synthase and cytochrome f/b_6 complexes are dependent on the accumulation of all the subunits within each particular complex but are independent of one another (Rochaix, 1992; Barkan et al., 1995). Thus, the level of any particular subunit should reflect the integrity of the complex as a whole. If BSD2 plays a general role in complex assembly or chloroplast translation, then components of the ATP synthase and cytochrome f/b_6 complexes should be reduced in *bsd2* plants.

As shown in Figure 8A, proteins encoding components of both the ATP synthase (CF1α) and the cytochrome f/b_6 complex (cytochrome *f* and subunit IV) accumulated to similar levels in both mutant and wild-type plants grown under low light conditions. Thus, BSD2 does not appear to be essential for the accumulation or assembly of the ATP synthase and cytochrome f/b_6 complexes in chloroplasts. Furthermore, the nuclear-encoded proteins LHCPII and a chloroplast-encoded subunit of the NAD(P)H dehydrogenase (NDH-H) also accumulated to wild-type levels in low-light-grown *bsd2* mutants. Notably, under moderate light conditions, the levels of most of these proteins decreased in mutant plants. This decrease was particularly striking for NDH-H, which localizes preferentially to bundle sheath cells in the closely related C_4 grass sorghum (Kubicki et al., 1996). Assuming a similar pattern of expression in maize, the decreased levels of NDH-H in *bsd2* mutants may reflect the severe disruption of bundle sheath cell chloroplast ultrastructure seen when plants are grown under moderate light conditions (Roth et al., 1996). Together, these findings indicate that BSD2 does not play a general role in chloroplast translation or in the accumulation and assembly of several photosynthetic complexes within the chloroplast.

To look at the role of BSD2 in chloroplast import, we also examined C_4 photosynthetic enzyme accumulation patterns. Pyruvate orthophosphate dikinase, NAD(P)–malate dehydrogenase, and NAD(P)–malic enzyme are nucleus-encoded proteins that are targeted to the chloroplast stroma. The accumulation of these proteins to similar levels in mutant and wild-type leaf tissue (Figures 8B and 8C) suggested that correct chloroplast targeting and processing occurs in both bundle sheath and mesophyll cells of *bsd2* plants. Furthermore, because the enzymatic activities of pyruvate orthophosphate dikinase, NAD(P)–malate dehydrogenase, and

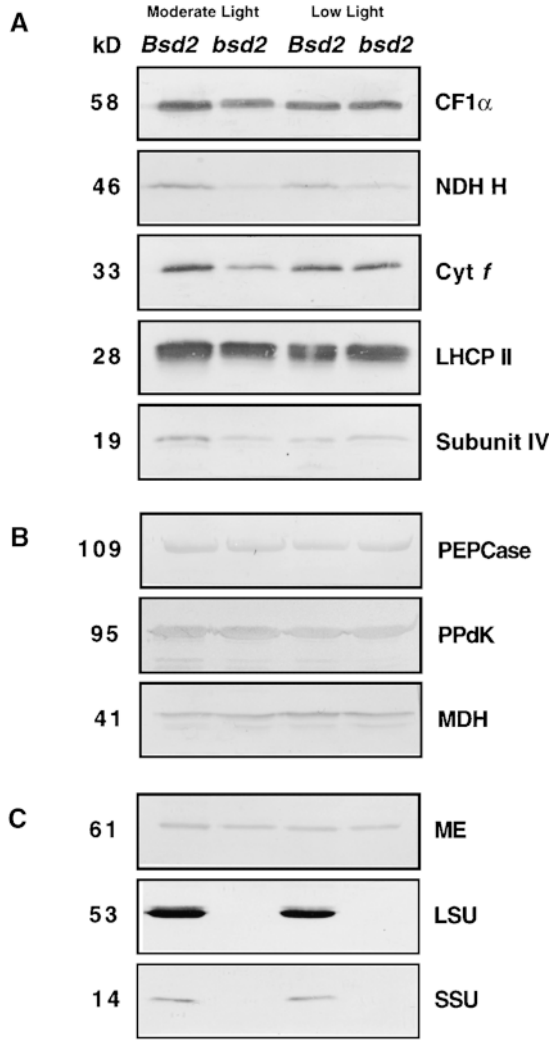

Figure 8. Immunoblot Analysis of Nucleus- and Chloroplast-Encoded Proteins in Wild-Type (*Bsd2*) and Mutant (*bsd2*) Plants.

Protein was isolated from plants grown under moderate (100 μmol m^{-2} sec^{-1}) or low (10 μmol m^{-2} sec^{-1}) light conditions. Blots were challenged with antisera raised against the following proteins. Molecular weights are indicated at left in kiloDaltons (kD).

(A) Components of the photosynthetic electron transport chain. Cyt, cytochrome.

(B) Mesophyll cell–specific C_4 photosynthetic enzymes: phosphoenolpyruvate carboxylase (PEPCase), pyruvate orthophosphate dikinase (PPdK), and NAD(P)–malate dehydrogenase (MDH).

(C) Bundle sheath cell–specific C_4 photosynthetic enzymes: NAD(P)–malic enzyme (ME) and the LSU and SSU of Rubisco.

NAD(P)–malic enzyme are similar in both wild-type and mutant *bsd2* plants (Smith et al., 1998), these nuclear-encoded C_4 enzymes must be correctly assembled into active complexes. Thus, the failure to accumulate LSU and SSU proteins in *bsd2* mutants (Figure 8C) appears to be caused by a specific defect in Rubisco stability or assembly.

DISCUSSION

bsd2-m1 plants are characterized by a failure to accumulate both the large and small subunits of Rubisco. Previous studies with both higher plants (Rodermel et al., 1988, 1996) and algae (Schmidt and Mishkind, 1983; Spreitzer et al., 1985) have indicated that LSU and SSU protein accumulation is dependent on the synthesis or assembly of the Rubisco holoenzyme. When either SSU (Rodermel et al., 1988, 1996) or LSU (Schmidt and Mishkind, 1983; Spreitzer et al., 1985) synthesis is inhibited, there is a corresponding decrease in the accumulation of the other subunit. For example, in *RbcS* antisense tobacco plants, the decrease in LSU accumulation is proportional to the decrease in SSU levels (Rodermel et al., 1996). Furthermore, the decreased accumulation of LSU seems to result from a block in LSU translation due to decreased association of *rbcL* with polysomes (Rodermel et al., 1996).

Several lines of evidence suggest that the primary defect in *bsd2-m1* mutants is the misregulation of *rbcL* gene expression and not the misregulation of *RbcS* gene activity. First, steady state levels of *RbcS* transcripts are similar in dark-grown and light-shifted wild-type and *bsd2* mutant plants (Roth et al., 1996), whereas *rbcL* is aberrantly expressed in both dark- and light-grown mutants. Second, BSD2 is targeted to the chloroplast and is therefore unlikely to be involved in the transcriptional regulation or cytoplasmic synthesis of precursor SSU protein. Finally, by analogy with the *RbcS* antisense experiments, a limiting amount of SSU protein should result in a decrease in polysome-associated *rbcL* transcripts in *bsd2-m1* plants. Instead, most *rbcL* transcripts are associated with polysomes in the mutant. Together, these findings suggest that BSD2 is not directly involved in *RbcS* gene regulation.

The ectopic accumulation of *rbcL* transcripts in mesophyll cells of leaves of light-grown *bsd2* plants (Roth et al., 1996) as well as misexpression in dark-grown leaves suggest that BSD2 may regulate *rbcL* gene expression. Importantly, the levels of *rbcL* transcript in bundle sheath and mesophyll cells of leaves of *bsd2* plants are nearly identical (Roth et al., 1996), as are the levels of *rbcL* transcripts in dark-grown and light-shifted plants (Figure 5). Although increased transcription rates could account for the increased accumulation of *rbcL* transcripts in *bsd2* mutants relative to the wild type, it seems more likely that a defect in post-transcriptional regulation mediates these changes.

Support for the limited role of transcriptional rate in the control of plastid gene expression has come from studies of several chloroplast genes. Although transcription rates of individual chloroplast genes can vary greatly, the relative rates of transcription of most are maintained throughout chloroplast development (Deng and Gruissem, 1987). This suggests that the changes observed in steady state transcript levels of many plastid genes are mediated at the post-transcriptional level (reviewed in Rochaix, 1992). Furthermore, measurements of *rbcL* transcription rates in wild-type maize plants by using in vitro run-on assays suggest that the differential expression of *rbcL* in bundle sheath and mesophyll cells is mediated, in part, by post-transcriptional processes (Kubicki et al., 1994). Thus, the increased accumulation of *rbcL* transcripts in the mesophyll cells and in dark-grown *bsd2* plants is most likely due to the inability of mutant plants to destabilize *rbcL* transcripts. This suggestion is supported by the finding that *rbcL* transcripts are associated with polysomes in *bsd2-m1* mutant mesophyll cells. Previous studies have shown that ribosomes play an important role in stabilizing *rbcL* transcripts (Barkan, 1993) because *rbcL* transcripts are degraded when they are not associated with ribosomes.

The homology between BSD2 and DnaJ-like proteins has provided some insight into how BSD2 functions to regulate *rbcL* gene expression and protein synthesis. The DnaK (heat shock protein Hsp70) system of chaperones, including the DnaJ (Hsp40) and GrpE proteins, is an essential component of protein metabolism both in the cytosol and organelles (reviewed in Hartl, 1996). These proteins interact sequentially to prevent premature folding of nascent polypeptides and to transfer unfolded proteins to other chaperone systems (Szabo et al., 1994; Banecki and Zylicz, 1996). DnaJ acts first in this cycle, binding to nascent peptide chains and maintaining them in an unfolded state for transfer to DnaK (Szabo et al., 1994). Although BSD2 only shows similarity to DnaJ-like proteins over a limited domain, the functionality of this domain has been demonstrated in vitro (Szabo et al., 1996) and in vivo (Banecki et al., 1996). Using a rhodanese aggregation assay (Langer et al., 1992), Szabo et al. (1996) showed that the CRR of DnaJ was sufficient to prevent the aggregation of rhodanese through the formation of a protein–protein complex. The eight cysteines shared between BSD2 and the region of DnaJ responsible for preventing aggregation closely resemble the Zn binding domain of C4 Zn finger proteins. In DnaJ, these cysteines coordinate two Zn(II) ions (Banecki et al., 1996; Szabo et al., 1996). Notably, deletion of this cysteine-rich domain affects the in vitro binding of the DnaJ protein to substrates (Banecki et al., 1996; Szabo et al., 1996) and partially inhibits bacteriophage growth in vivo (Banecki et al., 1996). Therefore, the striking similarity between BSD2 and this domain of DnaJ suggests that BSD2 may play a role in preventing aggregation or misfolding of nascent polypeptides.

One possible scenario for BSD2 function is illustrated in Figure 9 and is based largely on a recent model of cyclic chaperonin function by Hartl (1996). As demonstrated by in vitro binding studies, DnaJ acts first in the chaperone cycle,

binding to nascent polypeptide chains (Langer et al., 1992). Thus, a chloroplast-localized DnaJ-like protein is likely to bind to LSU polypeptides as they emerge from the ribosome. Indeed, chloroplast-targeted DnaJ and GrpE-like proteins have recently been identified in pea (Schlicher and Soll, 1997). Based on the sequence similarity that BSD2 shares with DnaJ, we propose that BSD2 acts as an accessory protein to assist a DnaJ-like protein in maintaining LSU in an unfolded state. Because Rubisco accounts for more than half of the soluble protein in the chloroplast (Ellis, 1979), it is reasonable to envision the need for additional factors to prevent aggregation. It is predicted that the DnaJ–LSU–BSD2 complex then associates with a DnaK-like protein through interactions of the J domain of DnaJ, as previously outlined (Hartl, 1996). As recently demonstrated in *Escherichia coli*, the DnaK family of chaperones promotes the assembly of both bacterial and plant Rubisco (Checa and Viale, 1997). After an interaction with the nucleotide exchange factor, GrpE, DnaJ, DnaK, and BSD2 proteins would dissociate from the unfolded LSU protein, which is passed onto the chaperonin 60/chaperonin 21 (Cpn60/Cpn21) complex. Here, SSU and LSU complexes are assembled into the mature Rubisco holoenzyme (reviewed in Gutteridge and Gatenby, 1995; Hartl, 1996).

bsd2 plants do not accumulate Rubisco, despite an association of the *rbcL* transcripts with polysomes. According to our model, the absence of BSD2 would result in the aggregation of the nascent peptide chain. Once released, the aggregated protein would then be targeted for degradation. The lack of LSU protein would consequently cause SSU protein to be degraded. Although this model is consistent with our inability to detect Rubisco protein in mutant plants, it does not account for the ectopic accumulation of *rbcL* transcripts in mesophyll cells or for the increased levels of transcript observed in dark-grown tissue. One possible explanation is that the formation of LSU aggregates attenuates translation of polysome-bound mRNA. Ribosome pausing has been well documented in plant chloroplasts as a mechanism of translational control (Klein et al., 1988; Kim et al., 1994) that results in the accumulation of polysome-associated transcripts without accumulation of corresponding peptides (reviewed in Gillham et al., 1994). Thus, it is possible that in the absence of functional BSD2 protein, stalled ribosomes protect *rbcL* transcripts from degradation. Indeed, previous studies of maize mutants have indicated that polysome-associated *rbcL* transcripts are more stable than are unassociated transcripts (Barkan, 1993). Thus, increased levels of *rbcL* transcript present in dark-grown mutants and the ectopic polysome-associated *rbcL* transcripts in mesophyll cells of light-grown mutants may reflect an abnormally large pool of polysome-associated *rbcL* transcripts resulting from the block in LSU synthesis. In Chlamydomonas, several mutations have been described that block the accumulation of specific chloroplast-encoded proteins. Nevertheless, the transcripts encoded by these genes accumulate to similar or increased levels in the mutants relative to the wild type (Rochaix, 1992).

Although our model is highly speculative, experiments are under way to test several of the predictions generated. In particular, we have predicted a direct interaction of BSD2 with either a DnaJ-like protein or nascent LSU chains. Alternatively, BSD2 could be required for subsequent steps in LSU folding or assembly of the holoenzyme complex. We are currently generating polyclonal antibodies raised against BSD2 fusion proteins to define further the role of BSD2 in Rubisco assembly. It is interesting that despite many attempts, it is still not possible to assemble higher plant Rubisco in *E. coli*, even in cell lines overexpressing the known chaperonin proteins. This suggests that additional factors are required (reviewed in Gutteridge and Gatenby, 1995), and it is possible that BSD2 may be one such factor that is essential for higher plant Rubisco assembly.

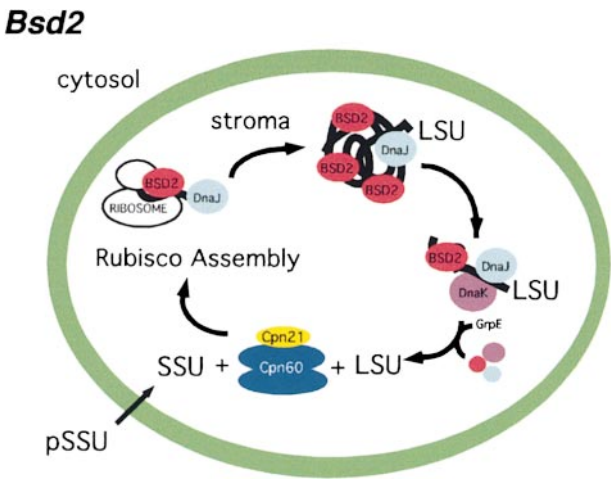

Figure 9. Model for BSD2 Action in Maize.

The model of chaperone action is based largely on the model of Hartl (1996; see text for details). As LSU polypeptides emerge from the ribosomes, BSD2 binds cooperatively with DnaJ-like proteins to prevent aggregation of nascent chains. The transfer of the DnaJ–LSU–BSD2 complex to a putative DnaK-like protein is mediated by the J domain of a DnaJ-like protein. Transfer of the LSU to the Cpn60/Cpn21 complex may be preceded by interactions with a GrpE-like protein. The precursor SSU (pSSU) is processed into the mature form (SSU) and, together with LSU, is assembled into the holoenzyme.

METHODS

Plant Material and Growth Conditions

Variegated *bsd2-m1* plants were outcrossed as males to the maize inbred line B73 (Pioneer Hi-Bred, Johnston, IA) and self-pollinated to generate F_2 populations. These F_2 progeny, segregating 3:1 wild-

type to stable pale green plants, were used for protein and RNA gel blot analyses. Selfed F_3 populations derived from the original variegated mutant were used in DNA gel blot analysis to examine segregation of *Mutator* (*Mu*)-hybridizing fragments with *bsd2-m1*. Mutant plants died soon after seed reserves were exhausted; therefore, seedling or third leaf tissue was used for DNA, RNA, and protein gel blot analyses. The *bz-mum9* allele was kindly provided by P. Chomet (DeKalb Plant Genetics, Mystic, CT) and contains a *Mu1* element in the *Bronze1* (*Bz1*) gene (Chomet et al., 1991).

To generate additional alleles of *bsd2*, we used two strategies. In collaboration with Pioneer Hi-Bred, we used a reverse genetics strategy to identify *Mu* insertions within *Bsd2* promoter and coding regions (TUSC). Although several putative insertions were identified, none of the putative insertions conferred a mutant phenotype. In the second strategy, pollen from a highly variegated homozygous *bsd2* plant was crossed onto ears of *Mu*-active plants. The ~3500 plants generated from these crosses were screened in a sand bench, and no pale green seedlings were identified.

For light-shift experiments, seedlings were grown in vermiculite at 28°C for 6 days in complete darkness. Plants were then either shifted to a 28°C growth chamber at the beginning of a 16-hr-light (180 μmol m^{-2} sec^{-1}) and 8-hr-dark cycle or left in darkness. After 24 hours, all tissue ~4 mm above the meristem was harvested and immediately frozen in liquid nitrogen. Etiolated tissue was harvested at the same time under a green safe light. We then returned plants to the growth chamber until mutant and wild-type individuals could be scored. Seedlings used for protein and RNA gel blot analyses were grown under moderate (100 μmol m^{-2} sec^{-1}) or low (10 μmol m^{-2} sec^{-1}) light at 28°C with 16 hr of light and 8 hr of darkness in a growth cabinet. Root tissue was harvested from plants grown in vermiculite; other tissue was harvested from plants grown in soil. Plastochron 1-5 tissue was collected by harvesting tissue 2 to 3 mm above the meristem before emergence of the first leaf from the coleoptile. The coleoptile was removed, and tissue was immediately frozen in liquid nitrogen. Plants were then returned to the growth chamber until wild-type and mutant phenotypes could be scored. For electron microscopy, third leaf sections were cut from greenhouse-grown plants and fixed, sectioned, and examined as previously described (Roth et al., 1996).

DNA Gel Blot and Linkage Analysis

DNA was isolated from wild-type and mutant siblings of several *bsd2-m1*–segregating families and from the progenitor lines kindly provided by W.F. Sheridan (University of North Dakota, Grand Forks). A two-step screening strategy was used to identify *Mu*-containing restriction fragments linked to the *bsd2* locus. In the first round of screening, DNA from three mutants and the two progenitor lines was digested with the following enzymes: SstI, EcoRI, SalI, PstI, XhoI, or HindIII. The DNA was size fractionated on agarose gels, blotted to a Zeta probe GT membrane (Bio-Rad), and hybridized as described previously (Brutnell and Dellaporta, 1994). Sets of filters were hybridized with *Mu* family–specific fragments for *Mu1*, *Mu1.7*, *Mu3*, *Mu5*, *Mu8*, and *MuDr* (Chandler and Hardeman, 1992) kindly provided by V. Chandler (University of Arizona, Tucson). Most *Mu*-containing restriction fragments identified were present in the progenitor lines or were not present in all the mutants. However, both SstI and PstI *Mu8*-specific restriction fragments were identified that were present in mutant but not progenitor plants. In the second round of screening, a total of 20 wild-type and 34 mutant plants from three different *bsd2-m1*–segregating families were examined to establish the close linkage relationship between *bsd2* and the *Mu8*-containing fragments. The linkage estimate was based on our inability to detect a single recombinant chromosome between the *Mu8* element and the *bsd2* locus in 34 mutant individuals from selfed populations (i.e., <1 recombinant per 68 chromosomes screened).

Gene Isolation and Cloning

Bsd2 sequences were isolated from genomic DNA according to Hall et al. (1998). Briefly, ~100 μg of DNA was digested with a threefold excess of restriction enzyme (Gibco BRL) and fractionated on an agarose gel. An ~1-cm-wide gel slice encompassing the fragments was excised, and the DNA was eluted and then purified with an Elutip-d column (Schleicher & Schuell). Fragments were ligated into plasmid pBluescript II KS+ and introduced into electrocompetent XL1 Blue MRF′ cells (Stratagene, La Jolla, CA).

Approximately 10,000 recombinant colonies were screened by hybridization for each clone. Clones were identified by colony hybridization (Sambrook et al., 1989) with either *Mu8*-specific (Mu8) or a full-length *Bsd2* cDNA clone (pB1.1). Genomic clones are shown in Figure 1. Because the SalI-SstI fragment from the mutant was unstable in pBluescript II KS+, sequences flanking the *Mu8* insertion were cloned into pTBP12 after polymerase chain reaction (PCR) amplification of genomic DNA by using a *Mu*-specific primer (P371; kindly provided by S. Dellaporta, Yale University, New Haven, CT) and the universal primer present in pBluescript II KS+.

A maize leaf cDNA library was kindly provided by A. Barkan (University of Oregon, Eugene). Screening and isolation of cDNA clones were performed as previously described (Hall et al., 1998).

DNA Sequence Analysis and Ligation-Anchored PCR

Plasmid subclones containing cDNA and genomic sequences shown in Figure 3 were fully sequenced on both strands by using a Sequenase kit (Amersham) or at an automated sequencing facility (MWG-Biotech, Ebersberg, Germany). Ligation-anchored PCR was performed as previously described (Troutt et al., 1992), with the following modifications. First-strand cDNA synthesis was initiated with the *Bsd2*-specific primer TBp15, using Superscript reverse transcriptase (Gibco BRL). The 3′ end of the anchor oligonucleotide was blocked with a primary amine and the 5′ end phosphorylated during primer synthesis (Genosys, Pampisford, UK). PCR amplification of the ligation reaction was performed with the TBp14 and T3 primers. Oligonucleotide primers were as follows: anchor oligonucleotide (5′-TTTAGTGAGGGTTAATAAGCGGCCGCGTCGTGACTGGGAGCGC-3′), T3 (5′-GCGGCCGCTTATTAACCCTCACTAAA-3′), TBp15 (5′-CCTTGGTCTTGATGCACAGG-3′), and TBp14 (5′-CTTGCAGTGGCGGGAGACGGG-3′). PCR-amplified products were cloned into the pGEM-T vector (Promega) and sequenced. BLAST (Altschul et al., 1990), PSORT (Nakai and Kanehisa, 1992), and BLASTP (Altschul et al., 1997) sequence searches were performed to define structural features of BSD2 and to identify putative *Bsd2*-like genes. These sequence data have been submitted to the GenBank database under accession number AF126742.

Purification of Separated Bundle Sheath and Mesophyll Cells

Bundle sheath cell strands and mesophyll cell protoplasts were isolated from wild-type B73 leaves as previously described (Hall et al., 1998).

Chloroplast Import Assay

Intact chloroplasts were isolated from *Pisum sativum* var Feltham First (Mould et al., 1991). A wheat germ cell-free lysate was used to translate mRNA derived by T3 RNA polymerase–driven transcription of a full-length *Bsd2* cDNA clone. Chloroplasts (50 μg of chlorophyll in a final volume of 125 μL) in 50 mM Hepes-KOH, pH 8.0, and 330 mM sorbitol, were preincubated with 8 mM MgATP for 10 min at 25°C in the light (60 μmol m^{-2} sec^{-1}). A ^{3}H-labeled BSD2 translation mixture (12.5 μL) was mixed with an equal volume of unlabeled leucine (5 mM final concentration) and added to the chloroplast suspension. Incubation was for 60 min in the light. To remove unbound proteins, we treated chloroplasts with 0.2 mg mL^{-1} thermolysin on ice. After protease treatment, chloroplasts were lysed in 10 mM Hepes and 5 mM $MgCl_2$, pH 8.0, for 5 min on ice. The envelope and thylakoid membranes were then separated from the stromal fraction by centrifugation at 15,000 rpm at 4°C for 10 min in a Biofuge 15R (Heraeus Instruments, Hanau, Germany). Stromal and thylakoid fractions were then run on a gel.

RNA Gel Blot Analysis

RNA was purified, electrophoresed on 1.2% formaldehyde–agarose gels, blotted onto Nytran membranes (Schleicher & Schuell), and hybridized as reported previously (Langdale et al., 1988a). The *Ppc1* (pTN1), *RbcS* (pJL10), *rbcL* (pJL12), *psbA* (pSD7), *Cab* (LHCP 1020), and ubiquitin (pSkuB1) cDNA clones have been described previously (Roth et al., 1996; Hall et al., 1998). A full-length *PorA* cDNA clone from barley (A7; Schulz et al., 1989) was kindly provided by K. Apel (Swiss Federal Institute of Technology, Zurich). This clone was digested with KpnI and BglII to yield a 3′ gene-specific fragment that was subcloned into pBluescript II KS+ and denoted *Por*.

Protein Gel Blot Analysis

Protein gel blot analysis was performed as previously described (Langdale and Kidner, 1994). Antisera raised against CF1α and cytochrome *f* and subunit IV were kindly provided by A. Barkan, and NAD(P)H dehydrogenase (NDH-H) antisera were provided by K. Steinmuller (Botanisches Institute der Ludwig-Maximilians-Universitat, Munich, Germany). Other antisera were as previously described (Roth et al., 1996). With the exception of large subunit antisera, all antibodies used were polyclonal.

Preparation of Polysomes

A procedure modified from that of Klaff and Gruissem (1991) was used to isolate total polysomes from leaf tissue. Light-grown seedling tissue (0.5 g) was ground in liquid nitrogen to a fine powder and added to 1.5 mL of buffer (Klaff and Gruissem, 1991). The homogenate was purified and adjusted to 0.5% sodium–deoxycholate, as described by Klaff and Gruissem (1991). Aliquots of 0.5 mL were layered onto 10.5 mL of 15 to 45% sucrose gradients in 40 mM Tris-HCl, pH 8.0, 20 mM KCl, 10 mM $MgCl_2$, 0.5 mg/mL heparin, and 100 μg/mL chloramphenicol and centrifuged for 150 min at 40,000 rpm in a Sorval (Du Pont) Ti 41 rotor at 4°C. Ten fractions of 650 μL were collected corresponding to the central region of the gradient. Fractions were adjusted to 0.5% SDS, 20 mM EDTA, and 80 mM Tris-HCl, pH 9.0. RNA was extracted with 1:1 phenol–chloroform and then 24:1 chloroform–isoamyl alcohol before precipitation with isopropanol. RNA was fractionated on agarose gels and hybridized with a fragment of maize chloroplast DNA (pZMC 460) containing both *rbcL* and *atpB* sequences (kindly provided by A. Barkan). Mesophyll cell protoplasts were isolated as described previously (Hall et al., 1998) from 5.0 g of seedling tissue and resuspended in 2.0 mL of polysome buffer (Klaff and Gruissem, 1991).

ACKNOWLEDGMENTS

We thank Colin Robinson (University of Warwick, UK) for help with chloroplast import experiments and Tim Nelson and Neil Schultes (Yale University, New Haven, CT) for providing field space for genetic experiments. We thank members of the laboratory for stimulating discussions and Miltos Tsiantis for critically reading the manuscript. We are grateful to Gülsen Akgün and Daphne Stork for excellent technical assistance, John Baker for photography, and Cledwyn Merriman for electron microscopy. This work was supported by grants to J.A.L. from the Biotechnology and Biological Sciences Research Council (BBSRC) and the Gatsby Charitable Foundation. T.P.B. is supported by a BBSRC David Phillips Fellowship. A.M. is supported by a BBSRC grant to Colin Robinson.

Received December 10, 1998; accepted February 20, 1999.

REFERENCES

Altschul, S.F., Gish, W., Miller, W., Myers, E.W., and Lipman, D.J. (1990). Basic local alignment search tool. J. Mol. Biol. **215,** 403–410.

Altschul, S.F., Madden, T.L., Schaffer, A.A., Zhang, J., Zhang, Z., Miller, W., and Lipman, D.J. (1997). Gapped BLAST and PSI-BLAST: A new generation of protein database search programs. Nucleic Acids Res. **25,** 3389–3402.

Banecki, B., and Zylicz, M. (1996). Real time kinetics of the DnaK/DnaJ/GrpE molecular chaperone machine action. J. Biol. Chem. **271,** 6137–6143.

Banecki, B., Liberek, K., Wall, D., Wawrzynow, A., Georgopoulos, C., Bertoli, E., Tanfani, F., and Zylicz, M. (1996). Structure–function analysis of the zinc finger region of the DnaJ molecular chaperone. J. Biol. Chem. **271,** 14840–14848.

Barkan, A. (1993). Nuclear mutants of maize with defects in chloroplast polysome assembly have altered chloroplast RNA metabolism. Plant Cell **5,** 389–402.

Barkan, A., and Martienssen, R.A. (1991). Inactivation of maize transposon *Mu* suppresses a mutant phenotype by activating an outward-reading promoter near the end of *Mu1*. Proc. Natl. Acad. Sci. USA **88,** 3502–3506.

Barkan, A., Voelker, R., Mendel, H.J., Johnson, D., and Walker, M. (1995). Genetic analysis of chloroplast biogenesis in higher plants. Physiol. Plant. **93,** 163–170.

Brutnell, T.P., and Dellaporta, S.L. (1994). Somatic inactivation and reactivation of *Ac* associated with changes in cytosine methylation and transposase expression. Genetics **138,** 213–225.

Brutnell, T.P., and Langdale, J.A. (1998). Signals in leaf development. In Advances in Botanical Research, Vol. 28, J.A. Callow, ed (London: Academic Press), pp. 162–195.

Chandler, V.L., and Hardeman, K.J. (1992). The *Mu* elements of *Zea mays*. Adv. Genet. **30,** 77–121.

Checa, S.K., and Viale, M. (1997). The 70-kDa heat-shock protein/DnaK chaperone system is required for the productive folding of ribulose-bisphosphate carboxylase subunits in *Escherichia coli*. Eur. J. Biochem. **248,** 848–855.

Chomet, P., Lisch, D., Hardeman, K.J., Chandler, V.L., and Freeling, M. (1991). Identification of a regulatory transposon that controls the *Mutator* transposable element system in maize. Genetics **129,** 261–270.

Deng, X.W., and Gruissem, W. (1987). Control of plastid gene expression during development: The limited role of transcriptional regulation. Cell **49,** 379–387.

Dengler, N.G., Dengler, R.E., Donnelly, P.M., and Filosa, M.F. (1995). Expression of the C_4 pattern of photosynthetic enzyme accumulation during leaf development in *Atriplex rosea* (Chenopodiaceae). Am. J. Bot. **82,** 318–327.

Edwards, G., and Walker, D.A. (1983). C3,C4: Mechanisms, and Cellular and Environmental Regulation, of Photosynthesis. (Oxford, UK: Blackwell Scientific Publications).

Ellis, R.J. (1979). The most abundant protein on earth. Trends Biochem. Sci. **4,** 241–244.

Fowler, J.E., Muehlbauer, G.J., and Freeling, M. (1996). Mosaic analysis of the *Liguleless3* mutant phenotype in maize by coordinate suppression of *Mutator*-insertion alleles. Genetics **143,** 489–503.

Gillham, N.W., Boynton, J.E., and Hauser, C.R. (1994). Translational regulation of gene expression in chloroplasts and mitochondria. Annu. Rev. Genet. **28,** 71–93.

Greene, B., Walko, R., and Hake, S. (1994). *Mutator* insertions in an intron of the maize *knotted1* gene result in dominant suppressible mutations. Genetics **138,** 1275–1285.

Gutteridge, S., and Gatenby, A.A. (1995). Rubisco synthesis, assembly, mechanism, and regulation. Plant Cell **7,** 809–819.

Hall, L., Rossini, L., Cribb, L., and Langdale, J.A. (1998). GOLDEN 2: A novel transcriptional regulator of cellular differentiation in the maize leaf. Plant Cell **10,** 925–936.

Hartl, F.U. (1996). Molecular chaperones in cellular protein folding. Nature **381,** 571–580.

Kelley, W.L. (1998). The J-domain family and the recruitment of chaperone power. Trends Biol. Chem. **6,** 222–227.

Kim, J., Klein, P.G., and Mullet, J. (1994). Synthesis and turnover of photosystem II reaction center protein D1. J. Biol. Chem. **269,** 17918–17923.

Klaff, P., and Gruissem, W. (1991). Changes in chloroplast mRNA stability during leaf development. Plant Cell **3,** 517–529.

Klein, R.R., Mason, H.S., and Mullet, J.E. (1988). Light-regulated translation of chloroplast proteins. I. Transcripts of *psaA-psaB*, *psbA*, and *rbcL* are associated with polysomes in dark-grown and illuminated barley seedlings. J. Cell Biol. **106,** 289–301.

Kubicki, A., Steinmuller, K., and Westhoff, P. (1994). Differential transcription of plastome-encoded genes in the mesophyll and bundle-sheath chloroplasts of the monocotyledonous NADP–malic enzyme—type C_4 plants maize and sorghum. Plant Mol. Biol. **25,** 669–679.

Kubicki, A., Funk, E., Westhoff, P., and Steinmüller, K. (1996). Differential expression of plastome-encoded *ndh* genes in mesophyll and bundle-sheath chloroplasts of the C_4 plant *Sorghum bicolor* indicates that the complex I–homologous NAD(P)H–plastoquinone oxidoreductase is involved in cyclic electron transport. Planta **199,** 276–281.

Langdale, J.A., and Kidner, C.A. (1994). *bundle sheath defective*, a mutation that disrupts cellular differentiation in the maize leaves. Development **120,** 673–681.

Langdale, J.A., Metzler, M.C., and Nelson, T. (1987). The *argentia* mutation delays normal development of photosynthetic cell types in *Zea mays*. Dev. Biol. **122,** 243–255.

Langdale, J.A., Rothermel, B.A., and Nelson, T. (1988a). Cellular patterns of photosynthetic gene expression in developing maize leaves. Genes Dev. **2,** 106–115.

Langdale, J.A., Zelitch, I., Miller, E., and Nelson, T. (1988b). Cell position and light influence C_4 versus C_3 patterns of photosynthetic gene expression in maize. EMBO J. **7,** 3643–3651.

Langdale, J.A., Hall, L.N., and Roth, R. (1995). Control of cellular differentiation in maize leaves. Philos. Trans. R. Soc. Lond. Ser. B **350,** 53–57.

Langer, T., Lu, C., Echols, H., Flanagan, J., Hayer, M.K., and Hartl, F.U. (1992). Successive action of DnaK, DnaJ and GroEL along the pathway of chaperone-mediated protein folding. Nature **356,** 683–689.

Martienssen, R., Barkan, A., Taylor, W.C., and Freeling, M. (1990). Somatically heritable switches in the DNA modification of *Mu* transposable elements monitored with a suppressible mutant in maize. Genes Dev. **4,** 331–343.

Martineau, B., and Taylor, W.C. (1985). Photosynthetic gene expression and cellular differentiation in developing maize leaves. Plant Physiol. **78,** 399–404.

Mayfield, S.P., Yohn, C.B., Cohen, A., and Danon, A. (1995). Regulation of chloroplast gene expression. Annu. Rev. Plant Physiol. Plant Mol. Biol. **46,** 147–166.

Meierhoff, K., and Westhoff, P. (1993). Differential biogenesis of photosystem II in mesophyll and bundle sheath cells of monocotyledonous NADP–malic enzyme—type C_4 plants: The non-stoichiometric abundance of the subunits of photosystem II in the bundle sheath chloroplasts and the translational activity of the plastome-encoded genes. Planta **191,** 23–33.

Moore, P.D. (1982). Evolution of photosynthetic pathways in flowering plants. Nature **295,** 647–648.

Mould, R.M., Shackleton, J.B., and Robinson, C. (1991). Transport of proteins into chloroplasts: Requirements for the efficient import of two lumenal oxygen-evolving complex proteins into isolated thylakoids. J. Biol. Chem. **266,** 17286–17289.

Mullet, J.E. (1988). Chloroplast development and gene expression. Annu. Rev. Plant Physiol. Plant Mol. Biol. **39,** 475–502.

Nakai, K., and Kanehisa, M. (1992). A knowledge base for predicting protein localization sites in eukaryotic cells. Genomics **14,** 897–911.

Nelson, T., Harpster, M., Mayfield, S.P., and Taylor, W.C. (1984). Light-regulated gene expression during maize leaf development. J. Cell Biol. **98,** 558–564.

Reinbothe, S., Reinbothe, C., Lebedev, N., and Apel, K. (1996). PORA and PORB, two light-dependent protochlorophyllide-reducing enzymes of angiosperm chlorophyll biosynthesis. Plant Cell **8,** 763–769.

Rochaix, J.-D. (1992). Post-transcriptional steps in the expression of chloroplast genes. Annu. Rev. Cell Biol. **8,** 1–28.

Rodermel, S.R., Abbott, M.S., and Bogorad, L. (1988). Nuclear-organelle interactions: Nuclear antisense gene inhibits ribulose bisphosphate carboxylase enzyme levels in transformed tobacco plants. Cell **55,** 673–681.

Rodermel, S., Haley, J., Jiang, C.-Z., Tsai, C.-H., and Bogorad, L. (1996). A mechanism for intergenomic integration: Abundance of ribulose bisphosphate carboxylase small-subunit protein influences the translation of the large-subunit mRNA. Proc. Natl. Acad. Sci. USA **93,** 3881–3885.

Roth, R., Hall, L.N., Brutnell, T.P., and Langdale, J.A. (1996). *bundle sheath defective2*, a mutation that disrupts the coordinated development of bundle sheath and mesophyll cells in the maize leaf. Plant Cell **8,** 915–927.

Sambrook, J., Fritsch, E.F., and Maniatis, T. (1989). Molecular Cloning: A Laboratory Manual. (Cold Spring Harbor, NY: Cold Spring Harbor Laboratory Press).

Santel, H.-J., and Apel, K. (1981). The protochlorophyllide holochrome of barley (*Hordeum vulgare* L.): The effect of light on the NADPH:protochlorophyllide oxidoreductase. Eur. J. Biochem. **120,** 95–103.

Schäffner, A., and Sheen, J. (1991). Maize *rbcS* promoter activity depends on sequence elements not found in dicot *rbcS* promoters. Plant Cell **3,** 997–1012.

Schlicher, T., and Soll, J. (1997). Chloroplast isoforms of DnaJ and GrpE in pea. Plant Mol. Biol. **33,** 181–185.

Schmidt, G.W., and Mishkind, M.L. (1983). Rapid degradation of unassembled ribulose 1,5-bisphosphate carboxylase small subunits in chloroplasts. Proc. Natl. Acad. Sci. USA **80,** 2632–2636.

Schulz, R., Steinmuller, K., Klaas, M., Forreiter, C., Rasmussen, S., Hiller, C., and Apel, K. (1989). Nucleotide sequence of a cDNA coding for the NADPH-protochlorophyllide oxidoreductase (PCR) of barley (*Hordeum vulgare* L.) and its expression in *Escherichia coli*. Mol. Gen. Genet. **217,** 355–361.

Sheen, J.-Y., and Bogorad, L. (1985). Differential expression of the ribulose bisphosphate carboxylase large subunit gene in bundle sheath and mesophyll cells of developing maize leaves is influenced by light. Plant Physiol. **79,** 1072–1076.

Sheen, J.-Y., and Bogorad, L. (1986a). Differential expression of six light-harvesting chlorophyll *a*/*b* binding protein genes in maize leaf cell types. Proc. Natl. Acad. Sci. USA **83,** 7811–7815.

Sheen, J.-Y., and Bogorad, L. (1986b). Expression of the ribulose-1,5-bisphosphate carboxylase large subunit gene and three small subunit genes in two cell-types of maize leaves. EMBO J. **5,** 3417–3422.

Smith, L.H., Langdale, J.A., and Chollet, R. (1998). A functional Calvin cycle is dispensable for the light activation of C_4 PEP-carboxylase kinase in the maize mutant *bsd2-m1*. Plant Physiol. **118,** 191–197.

Spreitzer, R.J., Goldschmidt-Clermont, M., Rahire, M., and Rochaix, J.-D. (1985). Nonsense mutations in the *Chlamydomonas* chloroplast gene that codes for the large subunit of ribulose bisphosphate carboxylase/oxygenase. Proc. Natl. Acad. Sci. USA **82,** 5460–5464.

Szabo, A., Langer, T., Schröder, H., Flanagan, J., Bukau, B., and Hartl, F.U. (1994). The ATP hydrolysis-dependent reaction cycle of the *Escherichia coli* Hsp70 system—DnaK, DnaJ, and GrpE. Proc. Natl. Acad. Sci. USA **91,** 10345–10349.

Szabo, A., Korszun, R., Hartl, F.U., and Flanagan, J. (1996). A zinc finger-like domain of the molecular chaperone DnaJ is involved in binding to denatured protein substrates. EMBO J. **15,** 408–417.

Taylor, W.C. (1989). Regulatory interactions between nuclear and plastid genomes. Annu. Rev. Plant Physiol. Plant Mol. Biol. **40,** 211–233.

Tobin, E.M., and Silverthorne, J. (1985). Light regulation of gene expression in higher plants. Annu. Rev. Plant Physiol. Plant Mol. Biol. **36,** 569–593.

Troutt, A.B., McHeyzer-Williams, M.G., Pulendran, B., and Nossal, G.J.V. (1992). Ligation-anchored PCR: A simple amplification technique with single-sided specificity. Proc. Natl. Acad. Sci. USA **89,** 9823–9825.

Viret, J.-F., Mabrouk, Y., and Bogorad, L. (1994). Transcriptional photoregulation of cell-type preferred expression of maize *rbcS*-m3: 3′ and 5′ sequences are involved. Proc. Natl. Acad. Sci. USA **91,** 8577–8581.

Wang, J.-L., Turgeon, R., Carr, J.P., and Berry, J.O. (1993). Carbon sink-to-source transition is coordinated with establishment of cell-specific gene expression in a C4 plant. Plant Cell **5,** 289–296.